Ni−V$_2$O$_5$·nH$_2$O Core−Shell Nanocable Arrays for Enhanced Electrochemical Intercalation

Katsunori Takahashi,[†,‡] **Ying Wang,**[†] **and Guozhong Cao*,**[†]

*Materials Science and Engineering, University of Washington, 302 Roberts Hall Box 352120,
Seattle, Washington 98195, and Steel Research Laboratory, JFE Steel Corporation, Kawasaki-cho,
Chuo-ku, Chiba 260-0835, Japan*

Received: November 15, 2004; In Final Form: December 3, 2004

We have prepared Ni−V$_2$O$_5$·nH$_2$O core−shell nanocable arrays for Li$^+$ intercalation applications. Ni−V$_2$O$_5$·nH$_2$O nanocables were prepared via formation of Ni nanorod arrays through the template based electrochemical deposition, followed by coating of V$_2$O$_5$·nH$_2$O on Ni nanorods through electrophoretic deposition. Transmission electron microscopy (TEM) micrograph clearly shows the Ni core was covered completely by a V$_2$O$_5$·nH$_2$O shell. Electrochemical analysis demonstrates that in a current density of 1.6 A/g, the Li$^+$ intercalation capacity of Ni−V$_2$O$_5$·nH$_2$O nanocable array is approximately 10 times higher than that of single-crystal V$_2$O$_5$ nanorod array and 20 times higher than that of sol−gel-derived V$_2$O$_5$ film. Both energy density and power density of such nanocable-array electrodes are higher than the V$_2$O$_5$ film electrode by at least 1 order of magnitude. Such significant improvement in electrochemical performance is due to the large surface area and short diffusion path offered by the nanostructured V$_2$O$_5$·nH$_2$O.

Introduction. Electrochemical intercalation is used to store electroactive species based on fast reversible faradic reactions occurring at or near the surface of an intercalation compounds. An electroactive species in electrolyte is reduced at the surface and diffuses into the interior of the crystal structure of the intercalation compound, i.e., solid electrode, in response to an externally applied electric field.[1] Vanadium pentoxide (V$_2$O$_5$) is a typical intercalation compound with a layered structure,[2] and thus it is one of the most promising materials for applications in electrochemical pseudocapacitors and electrochromic smart windows because of its Li$^+$ intercalation ability.[3] In electrochemical pseudocapacitors, the amount of energy stored is proportional to the amount of the electroactive species that can be absorbed by the electrode. Electrochromic property arises from the change of valence state of vanadium through the intercalation process. For these applications, charge/discharge rate, intercalation capacity, and cycling fatigue resistance are the most important parameters. Since the diffusion coefficient of Li ion in V$_2$O$_5$ (10^{-12}−10^{-13} cm^2/s [4,5]) and electrical conductivity of V$_2$O$_5$ (10^{-2}−10^{-3} S/cm [6,7]) are rather small, the intercalation process is slow and only a surface layer is active in intercalation. Nanostructured materials possess large surface area (or a large surface-to-volume ratio) and a short diffusion distance and thus offer promises to achieve significantly enhanced intercalation capacity and faster intercalation/extraction kinetics.

One of the most promising nanostructures for intercalation applications is one-dimensional nanomaterials, such as nanowires, nanocables, and hollow tubes. Although various methods have been developed for the formation of nanorods or nanowires,[8] template-based synthesis is one of the most important fabrication methods for nanorod arrays, since this method offers the ability to fabricate unidirectionally aligned and uniformly sized nanorod arrays of a variety of materials. Martin et al.[9] investigated the electrochemical properties of vanadium pentoxide nanorod arrays made by filling vanadium oxide sol into porous polycarbonate (PC) membranes, and reported that nanorod arrays achieved 4 times the capacity of a thin-film electrode. We recently demonstrated single-crystal V$_2$O$_5$ nanorod arrays grown by electrochemical deposition, surface condensation induced by a change of local pH as a result of H$_2$O electrolysis, and sol−gel electrophoretic deposition, combined with template growth methods.[10,11] Single-crystal V$_2$O$_5$ nanorod-array electrode has 5 times higher energy storage density than sol−gel derived films in a current density of 0.7 A/g.[11,12] These results suggest that the specific surface area of electrode is important since the redox or intercalation reactions occur at and near the electrode interface with electrolyte; hence a nanorod array structure is effective for use as a capacitor.

Composite structures have also been explored to further enhance the intercalation properties of vanadium pentoxide. For example, a composite of V$_2$O$_5$ aerogel, and nickel fiber has been reported to achieve 80% of the theoretical capacity.[13] Kudo et al. demonstrated that a V$_2$O$_5$ gel and carbon composite has a capacity of 360 mAh/g with a high charge/discharge rate.[14] These results suggest that the characteristic distance of lithium diffusion and electrical conduction plays a significant role in determining the intercalation properties. In this paper, we investigated (1) the formation of Ni−V$_2$O$_5$·nH$_2$O cable arrays with Ni nanorod arrays coated by V$_2$O$_5$·nH$_2$O using sol electrophoretic deposition and (2) their electrochemical intercalation properties. Figure 1 shows a schematic illustrating the Ni−V$_2$O$_5$·nH$_2$O core shell nanostructure for electrochemical supercapacitors.

---

* Corresponding author. E-mail: gzcao@u.washington.edu. Fax: 206-543-3100.
† University of Washington.
‡ JFE Steel Corporation.

Letters

J. Phys. Chem. B, Vol. 109, No. 1, 2005 **49**
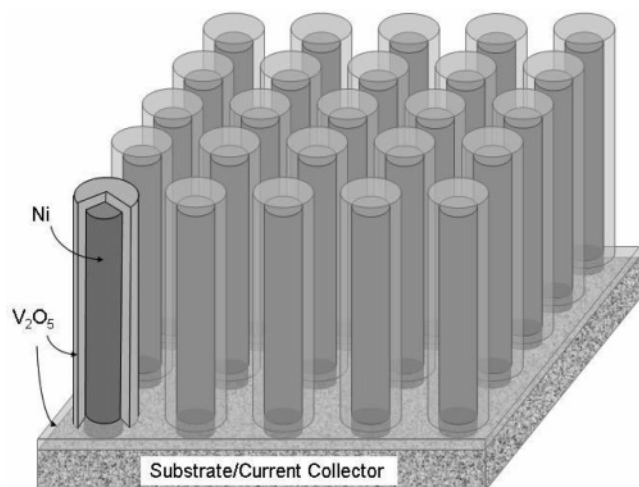
Figure 1. Schematic illustration of Ni$-$V$_2$O$_5$·nH$_2$O core shell structure as a capacitor electrode studied in the present investigation for improved performance.

Experimental Section. Ni$-$V$_2$O$_5$·nH$_2$O core$-$shell nanocable arrays were synthesized with two steps. Ni nanorod arrays were first grown by template-based electrochemical deposition. In the second step, hydrated vanadium pentoxide shell was deposited onto the surface of nickel nanorods through sol electrophoretic deposition. Ni nanorod arrays have been grown from commercial Ni plating solution NKBP11 (Caswell, Newark, NY) inside polycarbonate templates by electrochemical deposition. The templates used for this study were radiation track-etched hydrophilic PC membrane (Millipore, Bedford, MA) with pore diameters of 200 nm and thickness of 10 μm. To ensure a good electrical contact, the backside of the membrane template was first sputter-coated with Au$-$Pd before attaching it to the aluminum working electrode. Pt mesh was used as a counter electrode. The distance between two electrodes was kept at 25 mm. The applied voltage was 2.0 V, and the deposition lasted up to 3 h. Upon the completion of deposition, the samples were dried at 110 °C for 12 h in air. Dried samples were subsequently attached onto the titanium plate using silver paste. The samples with titanium plate were then immersed in methylene chloride to dissolve the PC membrane, resulting in the formation of free-standing Ni nanorod arrays attached on a titanium plate.

In the second step, the above Ni nanorod arrays were coated with a thin layer of V$_2$O$_5$·nH$_2$O by sol electrophoretic deposition. V$_2$O$_5$·nH$_2$O sols were synthesized using a method reported by Fontenot et al.[15] with V$_2$O$_5$ (Alfa Aesar) and 30% H$_2$O$_2$ (J. T. Baker) as precursors. V$_2$O$_5$ powder was dissolved in H$_2$O$_2$ solution with a V$_2$O$_5$ concentration of 0.15 M. The resulting solution has a H$_2$O$_2$/V$_2$O$_5$ ratio of 8:1. After stirring for 1.5 h at room temperature, the excess H$_2$O$_2$ was decomposed by sonication, and a yellow-brown gel was obtained. The resultant gel was then redispersed in DI$-$water, resulting in the formation of brownish sol, which contained 0.01 mol/L vanadium with a pH of 2.7. The primary vanadium species in the colloidal dispersion are hydrated vanadium oxide nanoparticles. From this sol, a thin layer of V$_2$O$_5$·nH$_2$O was coated onto Ni nanorods using electrophoretic deposition. Detailed description of the sol electrophoretic deposition process and setup have been reported previously.[16,17] The applied voltage was -0.8 V and the deposition lasted up to 15 min.

Ni$-$V$_2$O$_5$·nH$_2$O core$-$shell nanocable arrays were characterized by means of scanning electron microscopy (SEM, JEOL JSM-5200), transmission electron microscopy (TEM, Phillips

EM420), and X-ray diffractometry (XRD, Philips PW1830). Electrochemical properties of Ni$-$V$_2$O$_5$·nH$_2$O nanorod array electrode were investigated by a three-electrode cell. A 1 M LiClO$_4$ solution in propylene carbonate is used as electrolyte, and a Pt mesh is used as counter electrode with Ag/AgNO$_3$ as a reference electrode. A cyclic voltammetry and chronopotentiometric measurement were carried out by potentiostat/galvanostat (EG&G Princeton Applied Research, model 273).

Results and Discussion. Figure 2 shows typical SEM images of (a) Ni nanorod arrays grown in 200 nm PC membranes under an applied voltage of 2.0 V after PC membrane dissolved in methylene chloride and (b) Ni$-$V$_2$O$_5$·nH$_2$O core$-$shell nanocable arrays with a V$_2$O$_5$·nH$_2$O layer deposited under an applied voltage of -0.8 V. Ni nanorod arrays grown by electrochemical deposition have a diameter of ~200 nm and stand perpendicular to the substrate, and the XRD spectrum (not shown here) indicated that there is no other detectable phase other than Ni. The nanocables after the electrophoretic deposition in V$_2$O$_5$·nH$_2$O sol have a larger diameter than Ni nanorods, and each nanocable has an independent coating layer with a relatively smooth surface. In electrophoretic deposition, the electric field induces the oriented migration and stack of charged nanoclusters or nanoparticles on the growth surface, and no electrochemical reactions are required. However, Ni is oxidized to Ni^{2+} if the applied voltage is higher than -0.4 V in basic solution.[18] Ni^{2+} has a strong catalytic effect on the condensation reaction of V$_2$O$_5$·nH$_2$O sol and thus hinders the formation of homogeneous coating of V$_2$O$_5$·nH$_2$O on the surface of Ni nanorods. In the present study, -0.8 V (-0.44 V vs NHE) was applied on Ni nanorods to avoid possible dissolution of Ni.

Figure 2c shows a TEM micrograph of a Ni$-$V$_2$O$_5$·nH$_2$O core$-$shell nanocable. The image of nanocable consists of dark area in the center and light area outside along the axis. This morphology clearly suggests that the nanocable has a layered structure with different composition along the radial, and the dark area is likely to be Ni and the outer area be V$_2$O$_5$·nH$_2$O. Core material is covered completely and uniformly by V$_2$O$_5$·nH$_2$O shell with a thickness ranging from 30 to 50 nm based on SEM and TEM. It should be noted that the interface between Ni and V$_2$O$_5$·nH$_2$O is not smooth microscopically, which may be attributable to the Ni nanorod nature formed by electrochemical deposition. XRD analyses of nanocable arrays revealed the presence of Ni only. The V$_2$O$_5$·nH$_2$O coating is too thin to be detected, although EDS analyses unambiguously revealed the presence of vanadium. Figure 2d is the XRD pattern of the V$_2$O$_5$·nH$_2$O film grown by electrophoretic deposition from the same sol and identical voltage, suggesting the coating layer being V$_2$O$_5$·nH$_2$O.

Figure 3a compares the typical cyclic voltammograms of Ni$-$V$_2$O$_5$·nH$_2$O nanocable arrays and single-crystal V$_2$O$_5$ nanorod arrays (200 nm in diameter and 10 μm in length) using a scan rate of 10 mV/s; the synthesis and electrochemical properties of the latter have been reported in our previous publication.[12] The cyclic voltammogram of Ni$-$V$_2$O$_5$·nH$_2$O nanocable array shows cathodic peaks at -0.4 and -0.9 V, which are attributed to Li$^+$ intercalation, and anodic oxidation peaks at 0.0 and -0.6 V, which are attributed to Li$^+$ extraction. Single crystalline V$_2$O$_5$ nanorod array has cathodic reduction peaks at -0.3 and -0.9 V, and anodic oxidation peaks at 0.0 and -0.6 V (broad). Although the Li$^+$ extraction and intercalation behaviors were found similar in single-crystal V$_2$O$_5$ nanorod arrays and Ni$-$V$_2$O$_5$·nH$_2$O core$-$shell nanocable arrays, the charge capacity of Ni$-$V$_2$O$_5$·nH$_2$O core$-$shell nanocable array is about 10 times higher than that of a single-crystal V$_2$O$_5$ nanorod array and about
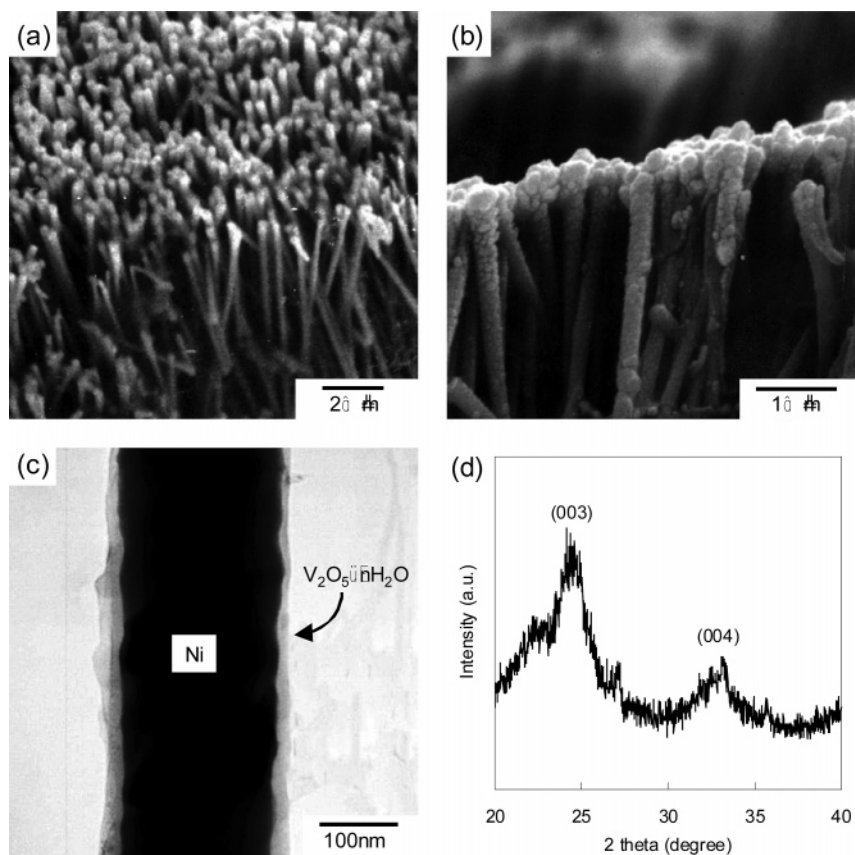
Figure 2. SEM image of (a) Ni nanorod arrays grown in 200 nm PC membranes under an applied voltage of 2.0 V and dissolving PC membrane in methylene chloride and (b) V_2O_5 coated Ni nanorods under an applied voltage of -0.8 V. (c) TEM micrograph of a Ni$-$$V_2O_5$ core$-$shell nanocable. (d) X-ray diffraction pattern of V_2O_5 film grown by sol electrophoretic deposition.

20 times higher than a V_2O_5 film at a given density. Our separate experiments have shown that the intercalation by Ni nanorod arrays was negligible under the experimental conditions; thus the enhancement is ascribed to both nanostructures and presence of water, which are to be discussed further later in this paper.

Figure 3b summarizes the Li^+ intercalation capacity as a function of current density of Ni$-$$V_2O_5 \cdot nH_2O$ nanocable arrays, single-crystal V_2O_5 nanorod arrays, and sol$-$gel derived V_2O_5 films. The capacity of Ni$-$$V_2O_5 \cdot nH_2O$ nanocable arrays is calculated based on a $V_2O_5 \cdot nH_2O$ thickness of 40 nm (average thickness) and density of 2.87 g/cm^3.[19] Although all three types of structures can achieve high intercalation capacity at a very lower current density, the intercalation capacity of both single-crystal V_2O_5 nanorod arrays and sol$-$gel films decreases rapidly as the current density increases. However, Ni$-$$V_2O_5 \cdot nH_2O$ nanocable arrays demonstrated high intercalation capacity at very high current densities. Ni$-$$V_2O_5 \cdot nH_2O$ nanocable arrays offer a significantly high charge and discharge rate. For example, in the case of current density of 1.6 A/g, core$-$shell nanocable arrays possess 10 times larger Li^+ intercalation capacity than that of V_2O_5 nanorod arrays and 20 times than that of sol$-$gel films. Such significantly improved transport property in Ni$-$$V_2O_5 \cdot nH_2O$ nanocable arrays can be attributed to both short mass transport distance and better electrical conduction. Although V_2O_5 has high capacity of lithium intercalation, it has both low diffusion coefficient of Li^+ in V_2O_5[4,5] and low electrical conductivity of V_2O_5.[6,7] These two characters limit the intercalation ability of V_2O_5 electrode and explain the fact that in both single-crystal nanorod arrays and sol$-$gel films, a high capacity can only be achieved at a very low current density and the intercalation capacity decreases rapidly as the current density increases. In the case of Ni$-$$V_2O_5 \cdot nH_2O$ core$-$shell

structure, Ni core acts as an electrode, resulting in a relatively large effective electric field applied on the thin $V_2O_5 \cdot nH_2O$ layer (shell). In addition, the $V_2O_5 \cdot nH_2O$ layer with a thickness of 30$-$50 nm offers a short diffusion distance for both Li ions and electrons.

The maximum capacity of Ni$-$$V_2O_5 \cdot nH_2O$ core shell nanocable array electrode is calculated as x in $Li_xV_2O_5$ equal to 3.1 based on 40 nm thickness of $V_2O_5 \cdot nH_2O$ layer. The capacity value with $x = 3.1$ (465 mAh/g) is higher than that of amorphous V_2O_5/carbon composite (360 mAh/g).[14] This high capacity might be explained by very short diffusion path in nanocomposite structure and the presence of H_2O in V_2O_5 crystal. The $I-V$ curve of Ni$-$$V_2O_5 \cdot nH_2O$ core$-$shell nanocable array electrode suggests that it may also consist of both pseudocapacitor and double-layer capacitor. Such hybrid phenomenon of both pseudocapacitor and double-layer capacitor was also observed in RuO_2/activated carbon[20] and V_2O_5/glassy carbon.[21] It is also known that $V_2O_5 \cdot nH_2O$ has better intercalation capacity than V_2O_5. Our separate experiments have demonstrated that sol$-$gel derived $V_2O_5 \cdot nH_2O$ films possess approximately 1.4 times higher intercalation capacity than that of sol$-$gel derived V_2O_5 films in a current density of 0.14 A/g as shown in Figure 4, which is in a good agreement with the literature.[22] It is obvious that the enhancement in electrochemical intercalation found in the nanocable arrays is mainly due to the nanostructures that provide large surface area and short diffusion distance. Figure 3c shows a Ragone plot for Ni$-$$V_2O_5 \cdot nH_2O$ nanocable, V_2O_5 nanorod, and sol$-$gel film. The specific energy (intercalation capacity) and specific power (intercalation and extraction rates) are calculated from chronopotentiograms.[13] This plot clearly demonstrates that Ni$-$$V_2O_5 \cdot nH_2O$ nanocable arrays have significantly enhanced specific energy (intercalation capacity) and specific power
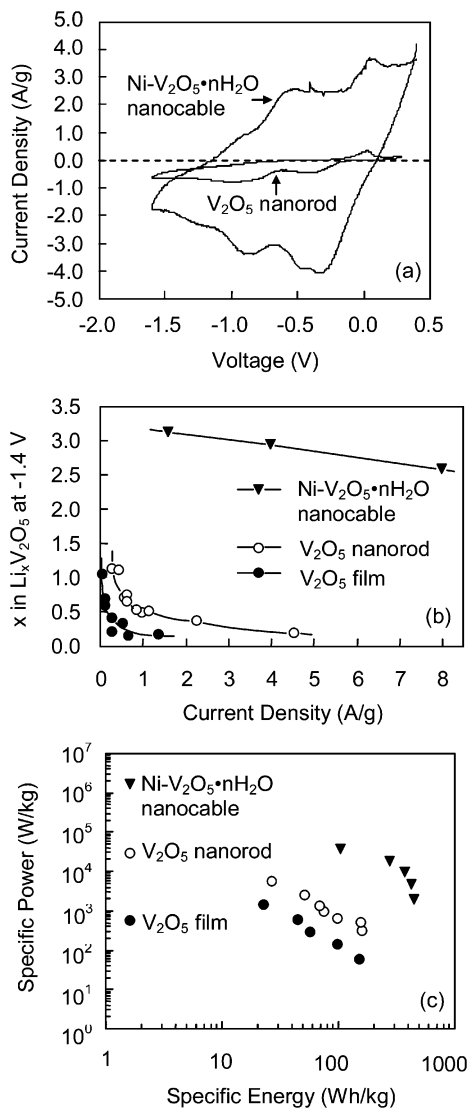
Figure 3. (a) Cyclic voltammograms of Ni−V$_2$O$_5$·nH$_2$O nanocable array and V$_2$O$_5$ nanorod array using a scan rate of 10 mV/s. (b) Relationship between current density and Li$^+$ insertion capacity of Ni−V$_2$O$_5$·nH$_2$O nanocable arrays, V$_2$O$_5$ nanorod arrays, and sol−gel films from chronopotentiometric measurements. (c) Ragone plot for Ni−V$_2$O$_5$·nH$_2$O nanocable array, V$_2$O$_5$ nanorod array, and sol−gel film.
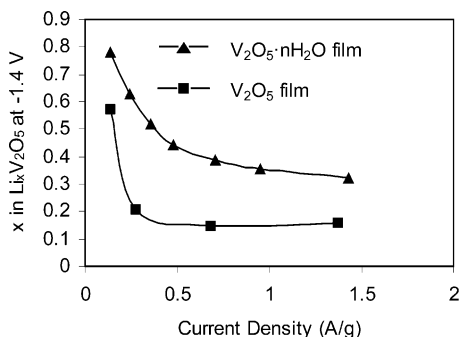
Figure 4. Relationship between current density and Li$^+$ insertion capacity of V$_2$O$_5$·nH$_2$O film and V$_2$O$_5$ film from chronopotentiometric measurements.

(intercalation kinetics) as compared with those of both single-crystal V$_2$O$_5$ nanorod arrays and sol−gel V$_2$O$_5$ film; the improvement has been at least 1 order of magnitude under comparable experimental conditions. It should be noted that although hydrated vanadium pentoxide possesses higher intercalation capacities than crystalline vanadium pentoxide, it may suffer from poor

cyclic performance, and the role of water in determination of the properties of the material remains unclear.[23] However, the enhancement of electrochemical intercalation properties in nanocable structure is beyond question and the concept and approach are directly applicable to other metal−oxide systems. The diameter of metal cores can be easily reduced by simply using templates with smaller pore, to achieve even larger surface area. This research is currently underway and will be reported separately later on.

Conclusions

Ni−V$_2$O$_5$·nH$_2$O nanocable arrays were achieved in two steps: first, Ni nanorod arrays were prepared through the template-based electrochemical deposition; then a coating of V$_2$O$_5$·nH$_2$O was applied over the Ni nanorods through electrophoretical deposition from the V$_2$O$_5$·nH$_2$O sol. The Ni core nanorod is covered completely and uniformly by a V$_2$O$_5$·nH$_2$O shell of average thickness of about 40 nm. In a current density of 1.6 A/g, Li$^+$ intercalation capacity of Ni−V$_2$O$_5$·nH$_2$O nanocable arrays is approximately 10 times higher than that of single-crystal V$_2$O$_5$ nanorod arrays and 20 times higher than that of sol−gel-derived V$_2$O$_5$ film. Both energy density and power density of such nanocable-array electrodes are higher than those of V$_2$O$_5$ film electrode by at least 1 order of magnitude. This significant improvement in electrochemical performance of Ni−V$_2$O$_5$·nH$_2$O nanocable arrays is ascribed to the large surface area and short diffusion distance provided by nanostructured V$_2$O$_5$·nH$_2$O.

References and Notes

(1) Conway, B. E. *Electrochemical Supercapacitors*; Plenum: New York, 1999.
(2) Legrand, A. P., Flandrois, S., Ed.; *Chemical Physics of Intercalation*; NATO Series B172; Plenum: New York, 1987.
(3) Murphy, D. W.; Christian, P. A.; Disalvo, F. J.; Waszczak, J. W. *Inorg. Chem.* **1985**, *24*, 1782.
(4) Portiron, E.; Salle, A. L.; Varbaere, A.; Piffard, Y.; Guyomard, D. *Electrochi, Acta* **1999**, *45*, 197.
(5) Lantelme, F.; Mantoux, A.; Groult, H.; Lincot, D. *J. Electrochem. Soc.* **2003**, *150*, A1202.
(6) Coustier, F.; Hill, J.; Owens, B. B.; Passerini, S.; Smyrl, W. H. *J. Electrochem. Soc.* **1999**, *146*, 1355.
(7) Livage, J. *Chem. Mater.* **1991**, *3*, 578.
(8) Cao, G. Z. *Nanostructures and Nanomaterials: Synthesis, Properties, and Applications*; Imperial College Press: London, 2004.
(9) Patrissi, C. J.; Martin, C. R. *J. Electrochem. Soc.* **1999**, *146*, 3176.
(10) Takahashi, K.; Limmer, S. J.; Cao, G. Z. *Proc. SPIE* **2003**, *5224*, 33.
(11) Takahashi, K.; Limmer, S. J.; Wang, Y.; Cao, G. Z. *Jpn. J. Appl. Phys.*, in press.
(12) Takahashi, K.; Limmer, S. J.; Wang, Y.; Cao, G. Z. *J. Phys. Chem. B* **2004**, *108*, 9795.
(13) Parent, M. J.; Passerini, S.; Owens, B. B.; Smyrl, W. H. *J. Electrochem. Soc.* **1999**, *146*, 1346.
(14) Kudo, T.; Ikeda, Y.; Watanabe, T.; Hibino, M.; Miyayama, M.; Abe, H.; Kajita, K. *Solid State Ionics* **2002**, *152−153*, 833.
(15) Fontenot, C. J.; Wiench, J. W.; Pruski, M.; Schrader, G. L. *J. Phys. Chem. B* **2000**, *104*, 11622.
(16) Limmer, S. J.; Seraji, S.; Forbess, M. J.; Wu, Y.; Chou, T. P.; Nguyen, C.; Cao, G. Z. *Adv. Mater.* **2001**, *13*, 1269.
(17) Limmer, S. J.; Seraji, S.; Forbess, M. J.; Wu, Y.; Chou, T. P.; Nguyen, C.; Cao, G. Z. *Adv. Funct. Mater.* **2002**, *12*, 59.
(18) Pourbaix, M. *Atlas of Electrochemical Equilibria in Aqueous Solution*; Pergamon Press: New York, 1966.
(19) Liu, Y. J.; Cowen, J. A.; Kaplan, T. A.; DeGroot, D. C.; Schindler, J.; Kannewurf, C. R.; Kanatzidis, M. G. *Chem. Mater.* **1995**, *7*, 1616.
(20) Dong, W.; Rolison, D. R.; Dunn, B. *Electrochem. Solid-State Lett.* **2000**, *3*, 457.
(21) Jang, J. H.; Han, S.; Hyeon, T.; Oh, S. M. *J. Power Sources* **2003**, *123*, 79.
(22) Park, H. K.; Smyrl, W. H.; Ward, M. D. *J. Electrochem. Soc.* **1995**, *142*, 1068.
(23) Wang, J.; Curtis, C. J.; Schulz, D. L.; Zhang, J. G. *J. Electrochem. Soc.* **2004**, *151*, A1.